An articulated raft-type wave energy converter

by I.F. Noad† and R. Porter*
University of Bristol, University Walk, Bristol, BS8 1TW, UK.
†imogen.noad@bris.ac.uk
*richard.porter@bris.ac.uk

Highlights:

• A novel solution method for the diffraction and radiation of waves by a floating, articulated raft is presented.
• Insight is given into how the device performance might be optimised.

1. Introduction

In this paper we are concerned with a three-dimensional model for a wave energy converter comprised of a series of floating rectangular pontoons. These are connected by a series of hinges, power being generated through the relative motions of adjacent elements due to the incident waves. The model, which assumes shallow draft and is analysed here using small amplitude linear water wave theory, is representative of the Cockerell raft design (e.g. [1]). The current interest in this problem is two-fold. First, we would like to develop an understanding as to what elements of raft-like wave energy converter design, more recently advocated in the development of the Pelamis device, allow it to generate power so successfully. In doing so we also hope to propose how to optimise the performance of raft-like designs. Second, it allows us to apply and extend some newly proposed mathematical techniques (see [5]) for the efficient solution to problems involving rigid plates lying on the surface of the water.

2. Formulation

Cartesian coordinates are chosen with the origin in the mean free surface level and z pointing vertically upwards. The fluid has density ρ and is of infinite depth, inviscid and incompressible. Fluid motions are irrotational and of small amplitude. A hinged raft of thickness h and density $\rho_s < \rho$ floats on the surface of the water with small draft $d = \rho_s h/\rho$. It is comprised of N rectangular sections as shown in Figure 1, each of width $2b$ and hinged along $x = X_n$ for $n = 1, ..., N-1$, $-b < y < b$. The entire raft is centred at the origin and occupies a region

$$\mathcal{D} = \bigcup_{n=1}^{N} \mathcal{D}_n \tag{1}$$

with

$$\mathcal{D}_n = \{(x, y) | X_{n-1} < x < X_n, -b < y < b\} \tag{2}$$

being the planform of the nth pontoon. Finally, we denote the total length of the raft by $2a = (X_N - X_0)$.

Monochromatic plane waves of radian frequency ω are incident from $x < 0$, making an anti-clockwise angle $\theta_0 \in (-\pi/2, \pi/2)$ with the positive x-direction. We shall assume waves of small steepness $KA \ll 1$ where A is the wave amplitude and $2\pi/K$ the wavelength where $K = \omega^2/g$ is the wave number and g is the gravitational acceleration. Damping devices placed along each hinge enable power take-off, exerting a force opposing and in proportion to the rate of change of angle Θ_n made between adjacent plates for $n = 1, ..., N-1$.

Under the assumptions made we describe the fluid velocity as the gradient of a scalar velocity potential,

$$\Phi(x, y, z, t) = \Re\left\{\frac{-igA}{\omega}\phi(x, y, z)e^{-i\omega t}\right\} \tag{3}$$

where $\phi(x, y, z)$ satisfies

$$\nabla^2\phi = 0 \qquad \text{on } z < 0 \tag{4}$$

and

$$|\nabla\phi| \to 0, \qquad z \to -\infty. \tag{5}$$

In addition, on $z = 0$ we have the combined kinematic and dynamic free surface condition

$$\phi_z(x, y, 0) = K\phi(x, y, 0) \tag{6}$$

for $(x, y) \notin \mathcal{D}$, and the kinematic condition on the raft

$$\phi_z(x, y, 0) = \frac{(x - X_{n-1})(\eta_n - \eta_{n-1})}{(X_n - X_{n-1})} \tag{7}$$

for $(x, y) \in \mathcal{D}_n$, $n = 1, ..., N$, where

$$\dot{\zeta}_n(x, y, z, t) = \Re\left\{A\eta_n(x, y, z)e^{-i\omega t}\right\} \tag{8}$$

are the vertical velocities of the hinges.

We exploit the linearity of the theory to decompose the motion of the raft into the sum of $N + 1$ linearly independent 'plate modes' (e.g. [3,4]) corresponding to the functions $f_n(x)$ for $n = 0, 1, ..., N$. There are two rigid body modes ($f_0(x)$ and $f_1(x)$, representing heave and pitch respectively) along with $N-1$ further hinged modes ($f_n(x)$ for $n = 2, ..., N$). These are defined by

$$f_n(x) = \begin{cases} 1 & \text{if } n = 0 \\ x & \text{if } n = 1 \\ |x - X_n| & \text{if } 1 < n \le N. \end{cases} \tag{9}$$

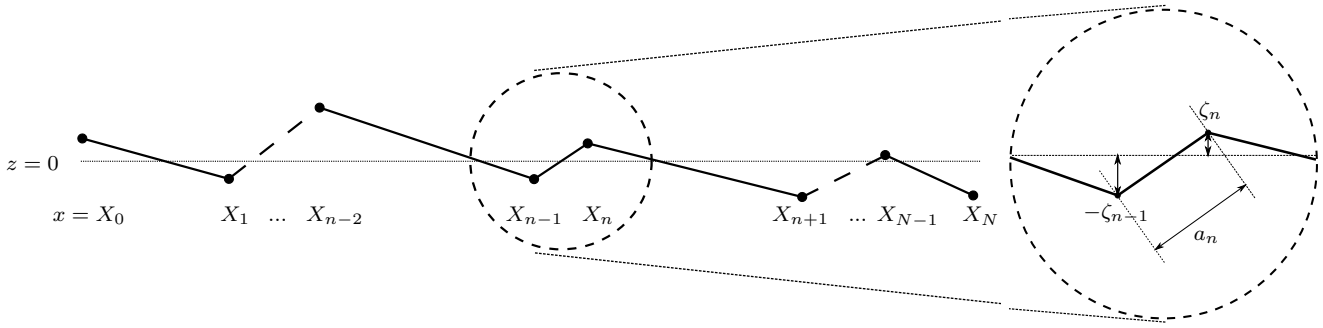

Figure 1: Some key parameters imposed on a side view (and close-up) of the articulated raft converter used in the hydrodynamic model.

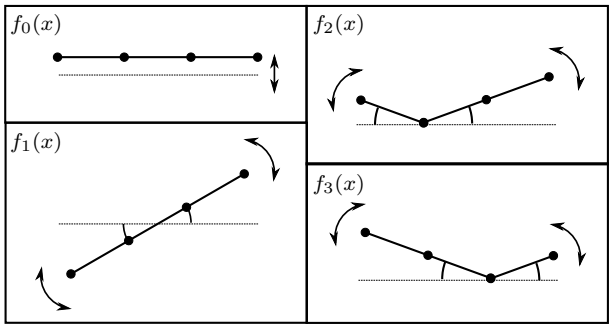

Figure 2: Illustration of 'plate modes' $f_n(x)$, $n = 0, 1, 2, 3$ for a raft made up of three pontoons.

For an illustration of the modes in the case of a raft made up of three components, see Figure 2. Thus, we may decompose our kinematic condition on the raft (7) as

$$\phi_z(x, y, 0) = \sum_{n=0}^{N} U_n f_n(x) \tag{10}$$

where U_0 is the vertical velocity of the heave mode and U_n, $n = 1, ..., N$ represent the angular velocities associated with the pitching and hinged modes. Under small amplitude theory they are given by

$$U_n = \begin{cases} \eta_0 & \text{if } n = 0 \\ \frac{\eta_N - \eta_{n-1}}{X_N - X_{n-1}} & \text{if } n = 1, ..., N. \end{cases} \tag{11}$$

This choice of modes is different to that proposed by Newmann [3,4] and suits our ultimate goal of assessing power production from hinged rafts as each mode engages just a single hinge. Correspondingly to the decomposition in (10) we write

$$\phi(x, y, z) = \phi^S(x, y, z) + \sum_{n=0}^{N} U_n \phi_n(x, y, z) \tag{12}$$

where $\phi^S(x, y, z)$ represents a scattering potential in which the raft is held fixed and is subject to an incident wave, it satisfies

$$\frac{\partial \phi^S}{\partial z}(x, y, 0) = 0 \qquad \text{for } (x, y) \in \mathcal{D} \tag{13}$$

and $\phi_n(x, y, z)$, for $n = 0, 1, ..., N$, represent radiation potentials associated with the forced motion of the raft in each of the $N + 1$ modes and satisfy

$$\frac{\partial \phi_n}{\partial z}(x, y, 0) = f_n(x) \qquad \text{for } (x, y) \in \mathcal{D}. \tag{14}$$

The incident wave is given by

$$\phi^I(x, y, z) = e^{iK(x \cos\theta_0 + y \sin\theta_0)} e^{Kz} \tag{15}$$

and the potentials ϕ^R and $\phi^D \equiv \phi^S - \phi^I$ describe outgoing waves at large distances from the raft.

The component of the hydrodynamic force due to scattering in the nth plate mode is defined as

$$X_n^S = i\omega\rho \iint_{\mathcal{D}} \phi^S(x, y, z) f_n(x)\, dx\, dy. \tag{16}$$

Similarly, we can define the force experienced in the nth mode due to forced motion in the mth mode in terms of the real added mass and radiation damping matrices $\mathbf{A}$ and $\mathbf{B}$, with components $\mathcal{A}_{mn}$, $\mathcal{B}_{mn}$, $m, n = 0, ..., N$, as

$$i\omega\mathcal{A}_{mn} - \mathcal{B}_{mn} = i\omega\rho \iint_{\mathcal{D}} \phi_m(x, y, z) f_n(x)\, dx\, dy. \tag{17}$$

Then the equation of motion of the raft can be written as

$$-i\omega\mathbf{M}\mathbf{U} = \mathbf{X}_S + (i\omega\mathbf{A} - \mathbf{B})\,\mathbf{U} + \mathbf{X}_e - \frac{i}{\omega}\mathbf{C} \tag{18}$$

where $\mathbf{M} = \text{diag}\{M_0, M_1, ..., M_N\}$ is a diagonal inertia matrix, $\mathbf{C}$ encodes the hydrostatic restoring forces, $\mathbf{X}_S = (X_0^S, X_1^S, ..., X_N^S)$ is the exciting force vector and

$$\mathbf{X}_e = -\mathbf{\Lambda}\mathbf{U} \tag{19}$$

with $\mathbf{\Lambda} = \text{diag}\{0, 0, \lambda_1, ..., \lambda_{N-1}\}$ represents the power take-off in the hinges, each having a damping rate λ_n, $n = 1, ..., N-1$. Elements of $\mathbf{C}$ are

$$\mathcal{C}_{nm} = \rho g \iint_{\mathcal{D}} f_n(x) f_m(x)\, dx\, dy \tag{20}$$

whilst

$$M_0 = 4\rho_s abh \tag{21}$$

and

$$\begin{aligned} M_n &= 2b\rho_s \int_{X_0}^{X_N} \int_{-d}^{h-d} (f_{n-1}^2(x) + z^2)\, dz\, dx \\ &\simeq 4\rho bda \left[\frac{4}{3}a^2 - (X_N - X_{n-1})(X_{n-1} - X_0)\right] \end{aligned} \tag{22}$$

for $n = 1, ..., N$ after elements of $O(h^3)$ have been negected due to small amplitude assumptions.

Assuming λ_n to be real constants for $n = 1, ..., N-1$ so that the power and velocity are in phase it may then be shown (see [2] for example) that the power can be written as

$$W = \frac{1}{2}\mathbf{X}_S^\dagger \mathbf{E}^\dagger \mathbf{\Lambda} \mathbf{E} \mathbf{X}_S \tag{23}$$

where $\mathbf{E} = (\mathbf{Z} + \mathbf{\Lambda})^{-1}$ and $\mathbf{Z} = \mathbf{B} - i\omega(\mathbf{M} + \mathbf{A} - \mathbf{C}/\omega^2)$ whilst the dagger denotes the conjugate transpose.

Case N=2: two pontoons

In the particular case of two identical pontoons this leads to

$$W = \frac{\left|\frac{Z_{02}}{Z_{00}} X_0^S - X_2^S\right|^2}{4(\Re\{z\} + |z|)} \left(1 - \frac{(\lambda_1 - |z|)^2}{|\lambda_1 + z|^2}\right) \tag{24}$$

where $z = Z_{22} - Z_{02}^2/Z_{00}$. We may then readily see that the raft is optimally tuned when $\lambda_1 = |z|$ giving

$$W_{max} = \frac{\left|\frac{Z_{02}}{Z_{00}} X_0^S - X_2^S\right|^2}{4(\Re e\{z\} + |z|)}. \tag{25}$$

Thus, in order to study the performance of the device we must first determine the hydrodynamic coefficients $\mathbf{A}$ and $\mathbf{B}$ along with the exciting force $\mathbf{X}_S$. These depend on the solution of the hydrodynamic problems for ϕ^S and ϕ_m, $m = 0, ..., N$ which is where our attention now turns.

3. Solution of the hydrodynamic problems

3.1 The scattering problem

The scattering problem deals with the diffraction of the incident wave when the raft is held fixed horizontally. We define the Fourier transform of $\phi^S(x, y, z)$ by

$$\overline{\phi}^S(\alpha, \beta, z) = \int_{-\infty}^{\infty} \int_{-\infty}^{\infty} \phi^D(x, y, z) e^{-i\alpha x} e^{-i\beta y}\, dx\, dy. \tag{26}$$

Then, taking Fourier transforms of (4), (5), it follows that

$$\left(\frac{d^2}{dz^2} - k^2\right) \overline{\phi}^S = 0 \qquad \text{for } z < 0 \tag{27}$$

where $k = \alpha^2 + \beta^2$ and $\overline{\phi}^D \to 0$ as $z \to -\infty$. Using (6), (7) we also find that

$$\left(\frac{d}{dz} - K\right) \overline{\phi}^S(\alpha, \beta, 0) = -K\overline{P}(\alpha, \beta) \tag{28}$$

where

$$\overline{P}(\alpha, \beta) = \iint_{\mathcal{D}} \phi^S(x, y, 0) e^{-i\alpha x} e^{-i\beta y}\, dx\, dy. \tag{29}$$

Thus, we find that the Fourier transformed velocity potential is given by

$$\overline{\phi}^S(\alpha, \beta, z) = \frac{K\overline{P}(\alpha, \beta)}{K - k} e^{kz}. \tag{30}$$

Invoking the inverse Fourier transform of (30) then results in an integral representation for $\phi^D(x, y, z)$

$$\phi^D(x, y, z) = \frac{K}{4\pi^2} \int_{-\infty}^{\infty} \int_{-\infty}^{\infty} \frac{\overline{P}(\alpha, \beta)}{K - k} e^{i\alpha x} e^{i\beta y} e^{kz}\, d\alpha\, d\beta. \tag{31}$$

Setting $z = 0$ then results in an integral equation for $\phi^S(x, y, 0)$ for $X_0 < x < X_N$ and $-b < y < b$. This may not be solved analytically, instead we employ a Galerkin expansion method using the approximation

$$\phi^S(x, y, 0) \simeq \sum_{p=0}^{2P+1} \sum_{r=0}^{2R+1} c_{pr}^S v_p\left(\frac{x}{a}\right) v_r\left(\frac{y}{b}\right) \tag{32}$$

where $v_r(t) = \frac{1}{2} e^{ir\pi/2} P_r(t)$ and $P_r(t)$ are orthogonal Legendre polynomials. Substituting for this approximation in the integral equation, multiplying through by $v_q^*(x/a) v_s^*(y/b)$ and integrating over $X_0 < x < X_N$, $-b < y < b$ results in the following system of linear equations

$$\begin{aligned} \frac{c_{qs}^S}{4(2q+1)(2s+1)} + \sum_{p=0}^{2P+1} \sum_{r=0}^{2R+1} c_{pr}^S K_{pqrs} \\ = j_q(Ka\cos\theta_0) j_s(Kb\sin\theta_0) \end{aligned} \tag{33}$$

for $q = 0, ..., 2P+1$ and $s = 0, ..., 2R+1$, where

$$K_{pqrs} = \frac{Kab}{4\pi^2} \int_{-\infty}^{\infty} \int_{-\infty}^{\infty} \frac{j_p(\alpha a) j_q(\alpha a) j_r(\beta b) j_s(\beta b)}{k - K}\, d\alpha\, d\beta \tag{34}$$

and j_n are spherical Bessel functions. Due to the symmetry properties of the j_n the integrals which determine K_{pqrs} vanish if either $p+q$ or $r+s$ is odd, a rendundancy which results in the reduction of (33) to a set of four uncoupled systems that may be solved for the unknown expansion coefficients c^S_{pr}.

The exciting torques on the raft may then be expressed in terms of the Galerkin expansion coefficients as

$$X^S_n = i\omega\rho ab \sum_{p=0}^{2P+1} c^S_{p0} g_{p,n} \tag{35}$$

where

$$g_{p,n} = \int_{-1}^{1} v_p(x) f_n(ax) dx, \tag{36}$$

an integral which may be expressed in closed form.

3.2 The radiation problem

The same solution method is applied to the radiation problem. This results in a different right hand side in the system of linear equations (33) due to the forcing provided by the incident wave being replaced by the forced oscillatory motion corresponding to each of the $N+1$ plate modes.

4. Preliminary results

Numerical work is ongoing, but preliminary results seem promising. These are shown in terms of the capture factor, a dimensionless measure of wave power absorption defined by

$$\hat{l} = \frac{W}{2b\,W_{inc}} \tag{37}$$

where $2b\,W_{inc}$ is the power incident on the width of the raft. Figure 3 shows results for a raft consisting of two identical pontoons plotted as a function of dimensionless wave number Ka for varying width to length ratios $a/b = 1, 2, 4, 8$. The curves in plot (a) show maximal capture factors and correspond to optimal tuning for every incident wave frequency. The capture factor is seen to increase in height with increasing a/b, suggesting an improvement in performance for longer devices. However, it is important to note that this is dependent on the choice of non-dimensionalisation of the power. Indeed, if we had non-dimensionalised using the volume instead then the improvement would be less significant.

The peaks in the curves suggest resonance for wavelengths of about twice the device length $\lambda = 2\pi/k \simeq 4a$. This means that, as you might expect, the raft bends maximally when half a wavelength covers the span of the raft.

Figure 3(b) shows results for a particular (as yet unoptimised) realisation of λ when $a/b = 8$. Only a small loss in power absorption is seen when the device is tuned to a particular incident wave frequency.

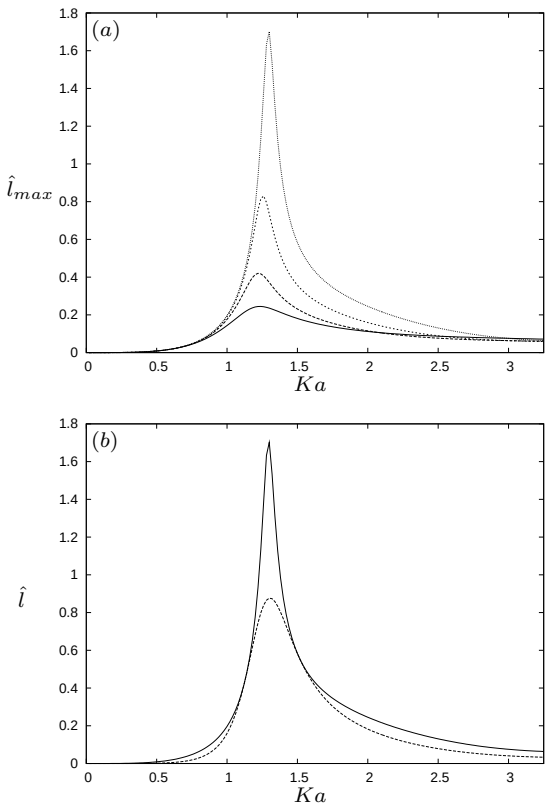

Figure 3: Capture factor is plotted as a function of Ka for a raft of two identical pontoons subject to normally incident waves. (a) shows maximal capture factors for varying length to width ratios $a/b = 1, 2, 4, 8$ corresponding to the solid, dashed, dotted and chained curves respectively whilst (b) shows a particular realisation compared with the maximum when $a/2b = 8$. The density ratio ρ_s/ρ is set at 0.9.

Work is currently ongoing in producing numerical results for larger systems of pontoons.

References

1. Count, B.M., 1979, Exploiting wave power. *IEEE Spectrum* **16** 42-49.

2. Crowley, S.H., Porter, R. and Evans, D.V., 2013, A submerged cylinder wave energy converter. *J. Fluid Mechanics* **716** 566-596.

3. Lee, C.H. and Newman, J.N., 2000, An assessment of hydroelasticity for very large hinged vessels. *J. Fluids & Structures* **14** 957-970.

4. Newman, J.N., 2001, Wave effects on multiple bodies. *Hydro. in Ship & Ocean Eng.* **3** 3-26.

5. Porter, R., 2016, Surface wave interaction with rigid plates lying on water. *Submitted to Wave Motion.*